

IL-17A–producing resident memory $\gamma\delta$ T cells orchestrate the innate immune response to secondary oral *Listeria monocytogenes* infection

Pablo A. Romagnoli^a, Brian S. Sheridan^{a,b}, Quynh-Mai Pham^a, Leo Lefrançois^a, and Kamal M. Khanna^{a,c,1}

^aDepartment of Immunology, UCONN Health, Farmington, CT 06030; ^bDepartment of Molecular Genetics and Microbiology, Stony Brook University, Stony Brook, NY 11794-5120; and ^cDepartment of Pediatrics, UCONN Health, Farmington, CT 06030

Edited by Jason G. Cyster, University of California, San Francisco, CA, and approved June 10, 2016 (received for review January 15, 2016)

Memory $\gamma\delta$ T cells are important for the clearance of *Listeria monocytogenes* infection in the intestinal mucosa. However, the mechanisms by which memory $\gamma\delta$ T cells provide protection against secondary oral infection are poorly understood. Here we used a recombinant strain of *L. monocytogenes* that efficiently invades the intestinal epithelium to show that V γ 4⁺ memory $\gamma\delta$ T cells represent a resident memory (Trm) population in the mesenteric lymph nodes (MLNs). The $\gamma\delta$ Trm exhibited a remarkably static pattern of migration that radically changed following secondary oral *L. monocytogenes* infection. The $\gamma\delta$ Trms produced IL-17A early after rechallenge and formed organized clusters with myeloid cells surrounding *L. monocytogenes* replication foci only after a secondary oral infection. Antibody blocking studies showed that in addition to IL-17A, the chemokine receptor C-X-C chemokine receptor 3 (CXCR3) is also important to enable the local redistribution of $\gamma\delta$ Trm cells and myeloid cells specifically near the sites of *L. monocytogenes* replication within the MLN to restrict bacterial growth and spread. Our findings support a role for $\gamma\delta$ Trms in orchestrating protective immune responses against intestinal pathogens.

resident memory cells | $\gamma\delta$ T cells | intestinal immunity | infections

Lymphocytes that express the $\gamma\delta$ T-cell receptor (TCR) are typically found in small numbers in lymphoid tissues, but are highly enriched in mucosal epithelial barriers like the skin and respiratory, gastrointestinal, and reproductive tracts (1). They are the first type of T cells to appear early during development, populating each tissue in sequential waves as the fetus develops into a newborn (2). At this stage, invariant γ -chains expressed by $\gamma\delta$ T cells serve as hallmarks of residency as well as functionality in each of these tissues (3). However, new evidence suggests that $\gamma\delta$ T-cell function, particularly IL-17A production, may be imprinted at the time of their exit from thymus, regardless of the type of γ -chain expressed by these $\gamma\delta$ T cells (4). Nevertheless, resident $\gamma\delta$ T cells are located from birth in epithelial layers of mucosal tissues to rapidly respond to injury (5) or infections (6) to ensure the maintenance of homeostasis at mucosal barriers.

Immunological memory is an important protective mechanism for the host against pathogenic microbes, which allows the immune system to respond faster and more efficiently to a rechallenge with a defined pathogen. Several recent studies have shown that following a localized mucosal infection, a group of memory cells is generated that fails to recirculate, but preferentially resides in the mucosal tissues that served as the original site of infection (7). These resident $\alpha\beta$ TCR⁺ memory CD8 T cells are very important for providing protection during secondary infections (8, 9). Although a great deal is known about conventional memory CD8 $\alpha\beta$ T cells, our understanding of memory T-cell populations that express the $\gamma\delta$ TCR remains poor.

Evidence for $\gamma\delta$ T cells exhibiting memory-like properties was demonstrated more than a decade ago using nonhuman primates (10). However, investigation of the mechanisms that regulate memory $\gamma\delta$ T-cell development and function requires the use of murine models. Indeed, recently, using a mouse model of oral infection with recombinant *Listeria monocytogenes* containing a

modified Internalin A protein that mimics intestinal invasion in humans (11), we described a previously unreported population of protective memory $\gamma\delta$ T cells that were *L. monocytogenes* specific in the intestinal mucosa (12). More recently, several laboratories have identified memory $\gamma\delta$ T-cell populations in mice (13, 14). However, the precise mechanism by which these memory $\gamma\delta$ T cells confer protection remains unknown.

Listeria outbreaks recently have been particularly deadly, and understanding the protective mechanisms required to clear this pathogen will be critical for developing new therapies. *L. monocytogenes*-specific memory $\gamma\delta$ T cells preferentially express the V γ 4 chain (Garman nomenclature) and upon activation either produce IL-17A, IFN γ , or both cytokines (12). Whether these memory $\gamma\delta$ T cells exhibit qualities of resident memory is not known. Furthermore, the mechanisms by which the *L. monocytogenes*-specific memory $\gamma\delta$ T cells provide protection during a recall response remain to be determined. Thus, in this report we attempted to bridge these important gaps in our knowledge by using deep sequencing, parabiosis, flow cytometry, and imaging approaches. Our results show that the *L. monocytogenes*-elicited memory $\gamma\delta$ T cells form a resident memory population in the gut draining mesenteric lymph nodes (MLNs). Multiphoton dynamic microscopy showed that $\gamma\delta$ resident memory (Trm) population exhibited a strikingly static pattern of motility, which was radically changed upon rechallenge. In addition, we discovered several previously unidentified mechanisms by which these resident memory

Significance

Outbreaks of food-borne infections with *Listeria monocytogenes* can result in high mortality. Using a model of recombinant *L. monocytogenes* that models human infection in mice, we show that *L. monocytogenes*-specific memory $\gamma\delta$ T cells in fact represent a resident memory (Trm) population in the mesenteric lymph node that secrete IL-17A and cluster with *L. monocytogenes* replication foci after secondary infection. Furthermore $\gamma\delta$ Trms mediate the intranodal migration and redistribution of myeloid cells, which was necessary to contain the spread and growth of *L. monocytogenes*. Our findings demonstrate how $\gamma\delta$ Trm cells orchestrate pathogen-induced innate immune responses. These observations provide the rationale for designing novel vaccination strategies to harness the ability of $\gamma\delta$ Trm cells to provide protection against intestinal pathogens.

Author contributions: P.A.R., B.S.S., L.L., and K.M.K. designed research; P.A.R. and Q.-M.P. performed research; B.S.S. contributed new reagents/analytic tools; P.A.R. and K.M.K. analyzed data; and P.A.R. and K.M.K. wrote the paper.

The authors declare no conflict of interest.

This article is a PNAS Direct Submission.

Data deposition: The sequences reported in this paper have been deposited in the NCBI Sequence Read Archive: BioProject PRJNA299800 and BioSample SRP065262.

¹To whom correspondence should be addressed. Email: kkhanna@uchc.edu.

This article contains supporting information online at www.pnas.org/lookup/suppl/doi:10.1073/pnas.1600713113/-DCSupplemental.

cells protect the host from the spread of a mucosal challenge infection.

Results

***L. monocytogenes*-Elicited $V\gamma 4^+$ $\gamma\delta$ T Cells Form a Trm Population in MLNs Following Oral *L. monocytogenes* Infection.** At early time points following oral infection, recombinant *L. monocytogenes* invades intestinal mucosa and is later detected in the MLNs before it spreads systemically (15). Thus, we primarily focused our study on investigating $\gamma\delta$ T cells that reside in the gut-draining MLNs. Using our previously published model of oral infection (12), *L. monocytogenes*-immune mice were generated by infecting the animals with 2×10^9 cfu of a murinized strain of *L. monocytogenes*; the mice were considered at memory at 30^d postinfection (dpi). To investigate the migratory and functional signature of *L. monocytogenes*-elicited memory $\gamma\delta$ T cells in contrast to other $\gamma\delta$ T-cell populations, we performed deep sequencing of RNA (RNA-seq) extracted from sorted $V\gamma 1.1^+$ or $V\gamma 2^+$ or $V\gamma 1.1/2/3$ ($V\gamma 4^+$) $\gamma\delta$ T cells in the MLN at 9 dpi (the peak of the primary response), 30 dpi (memory), 1 d postoral *L. monocytogenes* recall (dpr), and 5 dpr (SI Appendix, Fig. S1A–F). Intriguingly, although *L. monocytogenes*-elicited $V\gamma 4^+$ $\gamma\delta$ T cells were located in the MLN, they did not express the typical LN homing genes such as Sell (L-Selectin, CD62L) or C-C chemokine receptor 7 (*ccr7*), which was in contrast to $V\gamma 1.1^+$ or $V\gamma 2^+$ $\gamma\delta$ T cells (SI Appendix, Fig. S1A). Conversely, $V\gamma 4^+$ $\gamma\delta$ T cells did exhibit increased expression of gut homing genes such as integrin $\beta 7$ (*itgb7*), and other chemokine receptors such as CCR2, CCR5, C-X-C chemokine receptor 3 (CXCR3), and CXCR6 (SI Appendix, Fig. S1C). Although *L. monocytogenes*-elicited $V\gamma 4^+$ $\gamma\delta$ T cells expressed sphingosine-1-phosphate receptor (S1PR1) and the transcription factor *klf2* (that are both involved in mediating recirculation of T cells) (16, 17), they also expressed high levels of CD69 (a known inhibitor of S1PR1) (18) that favors resident memory T-cell retention in tissues (19) (SI Appendix, Fig. S1A and C). With respect to $V\gamma 4^+$ $\gamma\delta$ T cells, protein expression analysis confirmed the RNA-seq data and also demonstrated the stark difference in phenotypic differences compared with naive $\alpha\beta$ T cells and the rest of the $\gamma\delta$ T-cell populations found in the MLN, including $V\gamma 1.1^+$, $V\gamma 2^+$, and $V\gamma 3^+$ $\gamma\delta$ T cells ($V\gamma 1.1/2/3$) (SI Appendix, Fig. S1H). To further characterize *L. monocytogenes*-elicited memory $\gamma\delta$ T cells as a bona fide resident T cell, we stained for the canonical markers of resident memory, CD69 and Integrin αE (CD103) (SI Appendix, Fig. S1H). We found that *L. monocytogenes*-elicited memory $\gamma\delta$ T cells are a heterogeneous population that expressed CD69 (>70%), but fail to express CD103 and S1PR1 (SI Appendix, Fig. S1H). Although $V\gamma 4^+$ memory $\gamma\delta$ T cells did not express the typical LN homing receptors, virtually the entire population expressed CXCR3 and CXCR6 (Fig. 1A). To test the hypothesis that the *L. monocytogenes*-elicited memory $V\gamma 4^+$ $\gamma\delta$ T cells are indeed resident memory cells, we performed parabiosis experiments in which Thy1.2⁺ *L. monocytogenes*-immune mice were joined to congenitally mismatched Thy1.1⁺ naive mice for 9–11 d before the mice were killed (20). We quantified Thy1.2⁺ naive $\alpha\beta$ CD4 T cells, $V\gamma 1.1/2/3$ $\gamma\delta$ T cells (which do not expand after *L. monocytogenes* infection), and memory $V\gamma 4^+$ $\gamma\delta$ T cells in the MLN as well as total $\gamma\delta$ T cells in the intraepithelial lymphocyte (IEL) compartment of *L. monocytogenes*-immune (red) vs. naive mice (blue) (Fig. 1A). Strikingly, in contrast to the percentage of circulating naive $\alpha\beta$ CD4 T cells or $V\gamma 1.1/2/3$ $\gamma\delta$ T cells, whose numbers in the MLN of both naive and *L. monocytogenes*-immune mice completely equilibrated after parabiosis, the percentage of *L. monocytogenes*-elicited memory $\gamma\delta$ T cells that migrated to the MLN of the naive parabiont mice was extremely small (~5% of the Thy1.2⁺ $V\gamma 4^+$ $\gamma\delta$ T cells). Similar to the $V\gamma 4^+$ $\gamma\delta$ T cells, the percentage of IEL resident $\gamma\delta$ T cells in *L. monocytogenes*-immune mice that migrated to the IEL compartment of the naive parabiont mice was very low (Fig. 1A). Because $V\gamma 4^+$ $\gamma\delta$ T cells failed to recirculate, the ratio of Thy1.2⁺ *L. monocytogenes*-elicited memory $\gamma\delta$ T cells was significantly lower than the ratio of Thy1.2⁺ naive $\alpha\beta$ CD4 T cells or

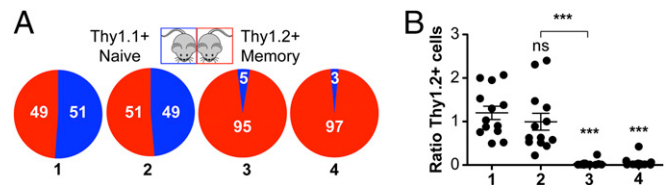


Fig. 1. *L. monocytogenes*-elicited $V\gamma 4^+$ $\gamma\delta$ T cells form a resident memory population in MLN following oral *L. monocytogenes* infection. (A) *L. monocytogenes*-immune mice (Thy1.2⁺) were surgically joined to naive mice (Thy1.1⁺) and maintained for 9 ($n = 9$) or 11 d ($n = 2$). Percentage of Thy1.2⁺ cells found in naive (blue) or *L. monocytogenes*-immune (red) host is shown. 1, naive CD4 $\alpha\beta$ T cells from MLN; 2, $V\gamma 1.1/V\gamma 2/V\gamma 3$ from MLN; 3, $V\gamma 4^+$ $\gamma\delta$ T cells from MLN; and 4, TCR β^- GL3⁺ CD3⁺ CD45⁺ found in the IEL compartment. (B) Ratio of absolute numbers of Thy1.2⁺ cells found in naive vs. *L. monocytogenes*-immune host after parabiosis. Data are expressed as mean \pm SEM analyzed by one-way ANOVA; *** $P < 0.0001$ calculated by Tukey's multicomparison test. Data are combined from three independent experiments. Each dot represents one pair of mice. All comparisons were made against naive CD4 $\alpha\beta$ T-cell ratios except when comparing $V\gamma 1.1/V\gamma 2/V\gamma 3$ vs. $V\gamma 4^+$ $\gamma\delta$ T cells in the MLN.

$V\gamma 1.1/2/3$ $\gamma\delta$ T cells recovered in the MLN of naive vs. *L. monocytogenes*-immune mice after parabiosis (Fig. 1B). We obtained similar results after parabiosis of Thy1-mismatched *L. monocytogenes*-immune mice (SI Appendix, Fig. S2), where both parabionts were previously infected with *L. monocytogenes*. In conclusion, our results strongly indicated that *L. monocytogenes*-elicited $V\gamma 4^+$ $\gamma\delta$ T cells in the MLN are indeed Trm cells.

Dynamics of Memory and Recalled $\gamma\delta$ Trm in the MLN. Although, the gene expression, phenotypic, and parabiosis data suggested that *L. monocytogenes*-elicited $V\gamma 4^+$ $\gamma\delta$ T cells indeed represent a Trm population, a hallmark of Trm cells is their restrictive motility patterns in tissues where they reside (21). Thus, next we assessed the motility patterns of naive, memory, and recalled $\gamma\delta$ T cells in vivo. We imaged explanted MLNs using two-photon (2P) microscopy and F1 mice generated by crossing BALB/c TCR δ -H2B-eGFP reporter (backcrossed from B6) (22) with BALB/c TCR $\alpha\beta$ -deficient mice to ensure a high-fidelity GFP expression only in $\gamma\delta$ T cells. As highlighted by singular tracks that correspond to individual $\gamma\delta$ T cells (SI Appendix, Fig. S3A and Movie S1), we observed that naive $\gamma\delta$ T cells (<1% are $V\gamma 4^+$ $\gamma\delta$ T cells) exhibited a normal random motility pattern. However, in stark contrast, $\gamma\delta$ T cells during the memory phase (30 dpi; >50% are $V\gamma 4^+$ $\gamma\delta$ T cells) displayed extremely limited motility and were strikingly static during the entire imaging period (SI Appendix, Fig. S3A and Movie S2). Upon reinfection, at 1 and 2 dpr, $\gamma\delta$ T cells were highly motile and some could be observed clustering together (SI Appendix, Fig. S3A and Movies S3 and S4; 1 dpr) (>50% $V\gamma 4^+$ T cells). The differences in track displacement at each time point are shown in Fig. 2A and SI Appendix, Fig. S3B. Other motility values such as the track length and the mean track speed of $\gamma\delta$ T cells in the MLN were also significantly different between naive (0 dpi), memory (30 dpi), or recall (1 and 2 dpr) (Fig. 2B and C), whereas the track straightness values showed no differences (Fig. 2D). To ensure that the differences in motility and speed that we observed were not due to the effect of the depth at which the $\gamma\delta$ T cells were localized within the MLN, we plotted the speed of the T cells against how far from the MLN capsule the cells were located at all times following infection. We found that there is little correlation between the mean track speed and the average distance from the capsule (SI Appendix, Fig. S3C). Therefore, we conclude that it is highly unlikely that the speed of *L. monocytogenes*-elicited $\gamma\delta$ T cells is significantly influenced by the location and depth of the cells within the MLN. These results clearly demonstrated that memory $\gamma\delta$ T cells exhibited a restrictive pattern of motility, very much akin to resident memory CD8 $\alpha\beta$ T cells (21). In addition,

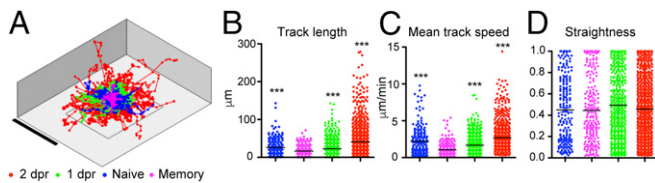


Fig. 2. Dynamics of memory and recalled $\gamma\delta$ Trm in the MLN. (A) Superimposed tracks of $\gamma\delta$ T cells from movies taken at different time points normalized to their starting coordinates. Magenta, 30 dpi (memory); blue, 0 dpi (naive); green, 1 dpr; and red, 2 dpr. (B) Track length. (C) Mean track speed. (D) Straightness data were obtained from 18 movies (naive = 3, memory = 5, 1 dpr = 5, and 2 dpr = 5). Each dot represents one cell and data are expressed as mean \pm SEM and analyzed by one-way ANOVA and Dunn's multicomparison test; *** $P < 0.001$.

$\gamma\delta$ Trm cells reacted immediately to accelerate and cluster in response to secondary infection in the MLN.

IL-17A-Producing $\gamma\delta$ Trm Cells Are Critical in the Rapid Control and Clearance of Bacteria Following Oral *L. monocytogenes* Rechallenge in the MLN. Our RNA-seq data showed a clear pattern of the transcriptional program followed by the *L. monocytogenes*-elicited $\gamma\delta$ Trm (SI Appendix, Fig. S1). Concordant with recent reports on IL-17A-producing $\gamma\delta$ T cells (23), *L. monocytogenes*-elicited $\gamma\delta$ Trm expressed the transcription factor Sox13 (SI Appendix, Fig. S1B). Moreover, these cells expressed the transcription factors ROR γ t (rorc), which together with ROR α (rora) induces the expression of IL-17A, IL-17F, and IL-22 (SI Appendix, Fig. S1B). In particular, the highest expression of IL-17A was observed at day 9 dpi and 5 dpr (SI Appendix, Fig. S1 D and E). In addition, the *L. monocytogenes*-elicited $\gamma\delta$ Trm cells expressed high levels of T-bet (tbx21) that mediates the expression of IFN γ (SI Appendix, Fig. S1 B, D, and E). The transcriptional profile also showed that the $\gamma\delta$ Trm cells could respond to several cytokines such as IL-2 (IL-2R α , IL-2R β , and IL-2R γ), IL-7 (IL-7R α and IL-2R γ), IL-18 (IL-18r1 and IL-18rap), and IL-23 (IL23r and IL12R β 1) (SI Appendix, Fig. S1D). Although *L. monocytogenes*-elicited V γ 4 $^{+}$ $\gamma\delta$ T cells can produce either IL-17A, IFN γ , or both upon oral *L. monocytogenes* rechallenge infection (12), the physiological significance of IL-17A produced by these cells during recall responses is not known. Thus, we first tested when these cytokines were produced by $\gamma\delta$ Trm cells as a correlate of their functional activity. *L. monocytogenes*-immune mice were reinfected with *L. monocytogenes* and approximately 19 h later, the mice were injected with 250 μg of brefeldin A i.v. At 5 h after brefeldin A injection, flow cytometric analysis showed that at 1 dpr *L. monocytogenes*-elicited V γ 4 $^{+}$ $\gamma\delta$ T cells in MLN primarily produced IL-17A, and a smaller percentage of cells secreted IFN γ , whereas a minor fraction was capable of producing both cytokines (Fig. 3A). Interestingly, at 1 dpr, the majority of the IL-17A-producing cells in the MLN were $\gamma\delta$ T cells (mostly $\gamma\delta$ Trm cells), and not CD4 or CD8 $\alpha\beta$ T cells (Fig. 3B). The importance of early IL-17A production by $\gamma\delta$ Trm cells was illustrated by the fact that IL-17A blockade resulted in increased bacterial burden, which significantly delayed clearance of *L. monocytogenes* compared with the isotype control antibody (Fig. 3C). These results demonstrated that the IL-17A produced by $\gamma\delta$ Trm cells was important for the rapid control and timely clearance of bacteria following oral *L. monocytogenes* recall in MLNs.

IL-17A-Producing $\gamma\delta$ Trm Cells Cluster at *L. monocytogenes* Replication Foci with Myeloid Cell Granulomas. To investigate the function of $\gamma\delta$ Trm cells in situ, MLNs were harvested following oral *L. monocytogenes* rechallenge and stained frozen sections were imaged using confocal microscopy. In *L. monocytogenes*-immune mice (~30 dpi), the majority of the $\gamma\delta$ T cells (>50% expressed the V γ 4 TCR) were located in the periphery of the MLN within the medullary (M) and interfollicular areas (IFAs), whereas a smaller percentage was found in the T-cell zone (T) (Fig. 4A, Upper Right). However, at 1 dpr, we observed a remarkable redistribution of $\gamma\delta$

T cells into defined clusters at the *L. monocytogenes* replication foci with CD11b $^{+}$ myeloid cells in the IFA of the MLN (Fig. 4 A, Upper Right and B, Left, white arrows). In our studies, we considered a "defined cluster" as a dense aggregate of cells and bacteria in which *L. monocytogenes* was packed in the center of a tight cluster of $\gamma\delta$ T cells and CD11b $^{+}$ cells. These clusters contained mostly $\gamma\delta$ Trm cells as evidenced by their ability to secrete IL-17A, which is mainly produced by a V γ 4 $^{+}$ $\gamma\delta$ T-cell subset after oral *L. monocytogenes* infection (Fig. 4B, Right) (12). This was further confirmed by staining of thick vibratome cut sections of MLNs for the $\gamma\delta$ TCR V γ 1.1, V γ 2, and V γ 3 chains (SI Appendix, Fig. S4 A and C-E). As shown in SI Appendix, Fig. S4A, we failed to observe any clusters of $\gamma\delta$ T cells that expressed the V γ 1.1, V γ 2, and V γ 3 TCR chains in the MLNs of memory or 1 dpr mice. Moreover, we did not observe the clustering of $\gamma\delta$ T cells in uninfected mice or at 1 dpi (primary infection; SI Appendix, Fig. S4B). This suggested that the redistribution and clustering was restricted to V γ 4 $^{+}$ $\gamma\delta$ Trm cells. We also quantified thick sections from F1 TCR δ -eGFP \times TCR $\alpha\beta$ reporter mice described above (SI Appendix, Fig. S4C) to confirm the numbers that were previously reported (12) (SI Appendix, Fig. S4D), and that V γ 4 $^{+}$ $\gamma\delta$ T cells preferentially locate to the IFA of MLNs (SI Appendix, Fig. S4E). Furthermore, $\gamma\delta$ T-cell clusters observed following oral *L. monocytogenes* reinfection dramatically increased in size at 2 and 3 dpr (SI Appendix, Fig. S5 A, B, and D). The clusters mostly disappeared by 5 dpr, by which time the $\gamma\delta$ T cells migrated primarily to the periphery of the MLN (SI Appendix, Fig. S5 A, B, and D). Interestingly, V γ 4 $^{+}$ $\gamma\delta$ T cells represented 95% of all $\gamma\delta$ T cells present in the MLN at 5 dpr (12). In addition, a great proportion of the CD11b $^{+}$ cells detected in the clusters were neutrophils as illustrated by Ly6G staining (SI Appendix, Fig. S5C). These results demonstrated that $\gamma\delta$ Trm cells participated in the secondary immune response to oral *L. monocytogenes* infection by forming clusters with myeloid cells at *L. monocytogenes* replication foci and by producing IL-17A.

Organized Redistribution and Cluster Formation of CD11b $^{+}$ Cells Is Dependent on IL-17A Production. To investigate what drove the formation of clusters, we tested whether IL-17A could be involved in the formation of clusters by recruiting myeloid cells that aggregate with the bacteria. *L. monocytogenes*-immune mice

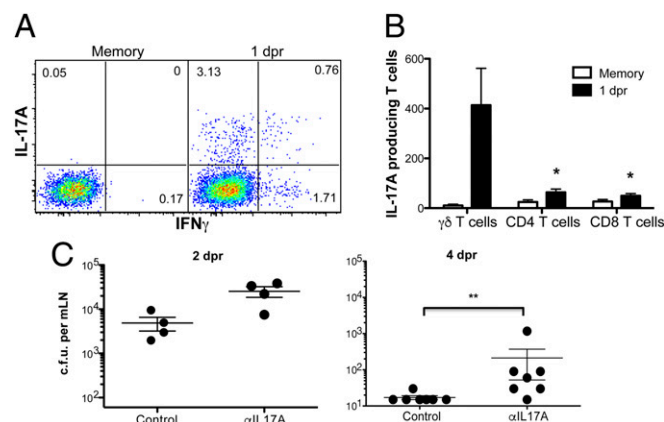


Fig. 3. IL-17A-producing $\gamma\delta$ Trm cells are critical in the rapid control and clearance of bacteria following oral *L. monocytogenes* rechallenge in MLN. (A) Frequency of IL-17A- and IFN γ -producing V γ 4 $^{+}$ $\gamma\delta$ T cells in vivo. Cells are gated on V γ 4 $^{+}$ $\gamma\delta$ T cells. Data are representative of three independent experiments, $n = 3$. (B) Absolute numbers of IL-17A-producing cells from MLN are shown. Data are combined from two independent experiments with $n = 3$ and expressed as mean \pm SEM and analyzed by one-way ANOVA test at each time point; * $P < 0.05$. (C) Cfu from MLN at 2 or 4 dpr after treatment with HRPN (control) or 17F3 (α IL-17A) antibody as described in Materials and Methods. Data are expressed as mean \pm SEM and analyzed by Student's t test; ** $P < 0.01$. Data shown are representative of two independent experiments, $n = 4-7$ mice per group.

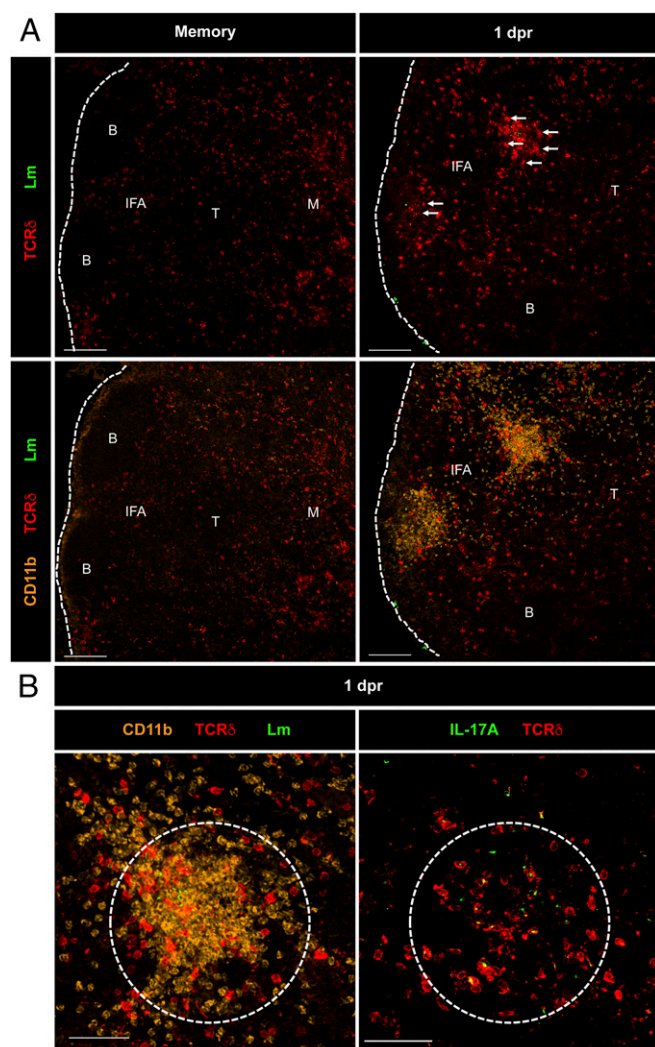


Fig. 4. IL-17A-producing $\gamma\delta$ Trm cells cluster at *L. monocytogenes* replication foci with myeloid cell granulomas. Sections of MLN from *L. monocytogenes*-immune (memory) (A, Left) or 1 dpr mice (A, Right) were immunostained for listeriolysin-O (LLO) (*L. monocytogenes*) or the indicated surface proteins or IL-17A (B). [Scale bars, 100 (A) and 50 (B) μm .] B, B-cell zone; IFA, interfollicular area; M, medulla; and T, T-cell zone.

were treated with isotype control (horseradish peroxidase, HRPN) or α IL-17A (17F3) antibodies during oral *L. monocytogenes* rechallenge and MLN sections were imaged. Strikingly, in contrast to control antibody treatment, the redistribution of CD11b⁺ cells into organized clusters in the MLN was impaired at 1 dpr when IL-17A was blocked (Fig. 5A). After 24 h (2 dpr), in control antibody-treated mice the CD11b⁺ cell clusters were larger, more organized, and denser, where the bacteria appeared to be localized and sequestered within the large myeloid granulomatous clusters (Fig. 5B, Left). In contrast, in IL-17A-blocked animals, the CD11b⁺ cell clusters in the MLN were more dispersed and disorganized, which likely resulted in the increased titers and spread of *L. monocytogenes* throughout the MLN (Fig. 5B, Right). Interestingly, at 1 dpr, the total numbers of myeloid cells (monocytes and neutrophils) recruited to the MLN were not decreased after IL-17A blockade (SI Appendix, Fig. S6); however, the redistribution of myeloid cells in organized granulomatous clusters was impaired. These data suggested that early production of IL-17A by $\gamma\delta$ Trm cells present at the *L. monocytogenes* replication foci mediated the intranodal migration and clustering of myeloid cells with the bacteria during rechallenge infection.

IL-17RA⁺ Myeloid Cells Are Critical for Bacterial Clearance. The role of neutrophils and inflammatory monocytes following a secondary oral *L. monocytogenes* infection (in the presence of preexisting immunity) is not well understood. Thus, to investigate the role of IL-17A and myeloid cells, we stained the single cell suspension of the MLN for IL-17RA. We found that the major population expressing the highest levels of IL-17RA was CD11b⁺ Ly6C^{hi} cells (SI Appendix, Fig. S7 A and B), consistent with inflammatory monocytes. To test their involvement in the clearance of bacteria after secondary oral *L. monocytogenes* infection, myeloid cells including monocytes and neutrophils were depleted using α Gr-1 antibody. We found that inflammatory monocytes were not only critical for bacterial clearance (SI Appendix, Fig. S7C) but also for the survival of mice following oral *L. monocytogenes* recall (SI Appendix, Fig. S7D).

IL-17A Regulates CXCL1 and CXCL9 Production in the MLN During Rechallenge Infection. Next we investigated the mechanism by which organized granulomatous clusters consisting of neutrophils, monocytes, and $\gamma\delta$ Trm cells formed in the MLN following rechallenge infection. Because it has been proposed that local changes in chemokine production can affect the distribution of immune cells within various LN compartments (24, 25), we first assessed the intranodal production of CXCL1, which is a potent neutrophil attractant in control antibody or anti-IL-17A-treated mice. Interestingly, in control antibody-treated mice, we observed the production of CXCL1, in areas surrounding *L. monocytogenes* replication foci and CD11b⁺ clusters in the MLN (SI Appendix, Fig. S8A). Because the $\gamma\delta$ Trm cells in MLN express high levels of CXCR3, we also stained for the CXCR3 ligand CXCL9 (SI Appendix, Fig. S8B). The geographical production of CXCL9 in the MLN was very similar to CXCL1, which conformed to the putative synergistic roles for these chemokines in mediating the local migration and localization of neutrophils and $\gamma\delta$ T cells during recall. Importantly, blocking IL-17A dramatically abrogated the production of both CXCL1 and CXCL9 in the MLN (Fig. 6D). Moreover, the lack of CXCL1 and CXCL9 production at the *L. monocytogenes* replication foci impaired the formation of organized clusters of CD11b⁺ myeloid and $\gamma\delta$ Trm cells (SI Appendix, Fig. S8 A and B). These results demonstrated that the redistribution of $\gamma\delta$ T cells and myeloid cells into organized granulomatous clusters was driven by IL-17A production, and IL-17A was important for regulating the local production of CXCL1 and CXCL9.

CXCR3 Enables the Local Redistribution and Migration of $\gamma\delta$ Trm Cells Near the Sites of *L. monocytogenes* Replication Within the MLN. The chemokine receptor CXCR3 can mediate the intranodal migration of T cells in LNs (24, 25). Since $\gamma\delta$ Trm cells expressed high levels of CXCR3 (SI Appendix, Fig. S1), and because high levels of CXCL9 were produced within *L. monocytogenes* replication foci (SI Appendix, Fig. S8B), we evaluated whether CXCR3 was important for the localization of $\gamma\delta$ Trm cells in the MLN after

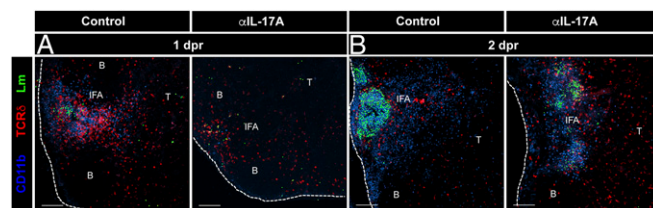


Fig. 5. Organized redistribution and cluster formation of CD11b⁺ cells is dependent on IL-17A production. *L. monocytogenes*-immune mice were recalled orally with *L. monocytogenes* and MLN sections at 1 dpr (A) or 2 dpr (B) were imaged. Mice were treated with HRPN (control) or 17F3 (α IL-17A) antibodies. Sections of MLN from *L. monocytogenes*-immune mice were immunostained for *L. monocytogenes* (rendered using Spot function of Imaris), GL3 (anti-TCR δ), and CD11b antibodies. Data are representative of two independent experiments, $n = 3$ mice. (Scale bars, 100 μm .)

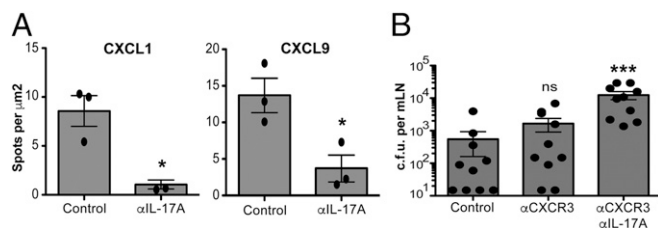


Fig. 6. CXCL1 and CXCL9 are expressed in clusters and CXCR3 drives cluster formation. (A) Numbers of spots per μm^2 quantified using Imaris software. Data are expressed as mean \pm SEM and analyzed by one-way ANOVA. Data are representative of two independent experiments, $n = 3$ per group; $*P < 0.05$. (B) Cfu at 4 dpr after treatment with HRPN + Armenian hamster IgGs (control), CXCR3-173 (αCXCR3), or CXCR3-173 and 17F3 ($\alpha\text{CXCR3} + \alpha\text{IL-17A}$) antibody. Data are expressed as mean \pm SEM and analyzed by one-way ANOVA; $***P < 0.001$. Data are representative of two independent experiments, $n = 7$ –10 mice per group.

recall. Moreover, we assessed whether the lack of $\gamma\delta$ Trm cell localization near *L. monocytogenes* replication foci would affect CD11b⁺ cell clustering and the overall formation of organized granulomatous structures. Indeed, blocking CXCR3 by antibody administration resulted in the disruption of $\gamma\delta$ Trm cell migration and clustering at the *L. monocytogenes* replication foci within the MLN at 1 dpr (SI Appendix, Fig. S9, Right). Interestingly, both $\gamma\delta$ T-cell and CD11b⁺ cell clustering around *L. monocytogenes* was impaired when CXCR3 was blocked (SI Appendix, Fig. S9, Right). The bacterial burden in the MLN after recall was higher in mice that received the CXCR3 antibody compared with the control antibody-treated mice (albeit not significantly, Fig. 6E). However, when both IL-17A and CXCR3 were blocked, bacterial burdens were significantly higher (on average 22-fold higher) compared with control antibody-treated mice (Fig. 6E). Notably, the bacterial burdens were 10-fold higher when only IL-17A was blocked (Fig. 3C), which suggested that both IL-17A and CXCR3 may function synergistically in regulating the intranodal migration and localization of $\gamma\delta$ Trm cells and CD11b⁺ myeloid cells during rechallenge infection. However, future studies will be needed to definitively prove the possible synergistic roles of CXCR3 and IL-17A in mediating pathogen clearance in the MLN following a secondary infection.

Discussion

The Internalin A mutant recombinant strain of *L. monocytogenes* provides an excellent means to model human *L. monocytogenes* infection in mice, because the modified Internalin A binds mouse E-cadherin with similar efficiency as the human counterpart (11). Using this model, we previously found the existence of *L. monocytogenes*-specific protective memory like $\gamma\delta$ T-cell population in mice (12). This finding begged the question as to what the mechanisms were by which *L. monocytogenes*-elicited memory $\gamma\delta$ T cells provided protection after challenge infection in the intestinal mucosa. Furthermore, it was not known whether these memory-like $\gamma\delta$ T cells represented a truly resident memory population. In the current report, we addressed these important questions.

By using parabiosis and 2P microscopy, we unexpectedly discovered that unlike resident memory CD8 T cells that are primarily located in nonlymphoid tissues, the V γ 4⁺ memory $\gamma\delta$ T cells represented a population of noncirculating memory cells that established residence in the gut-draining LNs. Gene and protein expression analysis showed that although these cells were located in the LNs, $\gamma\delta$ Trm failed to express CD62L and CCR7, but expressed CD69, CXCR3, and CXCR6. The chemokine receptor CXCR3 has previously been implicated in mediating CCR7-independent homing of activated CD8 T cells to reactive LNs (26). Because $\gamma\delta$ Trm cells did not express the typical LN homing receptors, the expression of CXCR3 likely allowed these cells to migrate to and remain in the LNs following infection.

Although CD69 is an early T-cell activation marker, it is also considered a hallmark of memory CD8 $\alpha\beta$ T-cell residency, which functions by inhibiting the expression of S1PR1 (19). Surprisingly, we found that even though $\gamma\delta$ Trm cells express CD69, they also express S1P receptors 1 and 4 as confirmed by RT-PCR (SI Appendix, Fig. S1G), suggesting that residency of $\gamma\delta$ Trm cells may be regulated differently compared with conventional $\alpha\beta$ Trm cells. Interestingly, $\gamma\delta$ Trm cells did not express CD103, which was in line with observations that showed that CD8 Trm cells found in secondary lymphoid organs and intestinal mucosa fail to express this marker (27).

We used TCR δ -H2B-eGFP reporter mice and MLN explants to show that $\gamma\delta$ Trm cells exhibited a unique motility program, characterized by remarkably limited movement in the cortical regions of the MLN under steady-state conditions. This movement mimicked the motility pattern exhibited by CD8 Trms in mucosal surfaces such as the skin (21). *L. monocytogenes*-elicited $\gamma\delta$ Trm cells had a high coefficient of arrest, which was in stark contrast to what was observed with naive $\gamma\delta$ T cells located in the cortical regions of the LN in unimmunized mice. Previous reports have investigated the motility patterns of naive $\gamma\delta$ T cells (28); however, the dynamics of memory $\gamma\delta$ T cells have not been described before. Memory $\gamma\delta$ Trm showed a restricted pattern of movement resembling that of sentinel cells that sense the environment and after a secondary infection respond immediately with rapid movement and clustering. Taken together, these results clearly demonstrated that the $\gamma\delta$ Trm cells represent a lymphoid resident memory cell population that exhibits a unique transcriptional profile and does not depend on CD103 expression or S1PR1 repression for establishing or maintaining residency.

We further showed that $\gamma\delta$ Trm cells were the primary producers of IL-17A early after secondary oral *L. monocytogenes* infection, and this production of IL-17A was important for the timely clearance of the bacteria. In line with our observations, populations of IL-17A-producing $\gamma\delta$ T cells with memory-like properties have been described in two recent reports after i.p. and skin infections (13, 29).

Whereas the protective mechanisms used by conventional memory CD8 $\alpha\beta$ T cells are better understood, little is known about how memory $\gamma\delta$ T cells enhance protection during secondary infections. After recall infection, CD8 Trm cells in the female reproductive tract secrete proinflammatory cytokines to alarm the innate arm of the immune system, resulting in rapid clearance of a secondary infection (30). Likewise, circulating memory CD8 T cells in the spleen respond similarly by activating inflammatory monocytes to assist in eliminating secondary *L. monocytogenes* challenge (31). Our findings illustrated for the first time to our knowledge the mechanisms by which $\gamma\delta$ Trm cells in the MLN mediate the rapid clearance of *L. monocytogenes* after a secondary challenge. We showed that immediately upon re-infection, $\gamma\delta$ Trm cells formed large clusters around the bacteria and secreted proinflammatory cytokine IL-17A, enabling the recruitment of myeloid cells such as neutrophils at the sites of *L. monocytogenes* replication foci and the formation of large organized granulomatous structures that facilitated timely bacterial clearance. Interestingly, the recruitment of myeloid cells to the MLN was not dramatically affected when IL-17A was blocked; however, the intranodal redistribution of myeloid cells such as neutrophils to the sites of *L. monocytogenes* replication foci was markedly affected. Nevertheless, it is difficult to completely isolate the effect of IL-17A blockade in the draining LN from the intestinal mucosa; thus, the possibility remains that some of the effect of blocking IL-17A on bacterial clearance may be related to the intestines. We found that inflammatory monocytes were also critical for controlling oral *L. monocytogenes* infection. Importantly, we showed that the monocytes expressed high levels of IL-17A, and thus were capable of responding to the IL-17A secreted by coclustering $\gamma\delta$ Trm cells.

A protective immune response is characterized by the large-scale migration of immune cells within and between lymphoid and peripheral tissues. This migration is carefully regulated by factors such as the organized secondary lymphoid structure and

the cellular expression of chemokine receptors and compartmentalized secretion of their cognate ligands. Recently, it has become clear that intranodal migration of immune cells plays a very important role in the rapid clearance of secondary infections (24, 25). CXCR3-mediated prepositioning and guidance is critical for the accelerated response by central memory CD8 $\alpha\beta$ T cells to secondary infections in the LNs (25). We observed that CXCR3 was highly expressed on $\gamma\delta$ Trm cells and antibody blocking of this receptor abrogated the local migration of $\gamma\delta$ Trm cells at the sites of *L. monocytogenes* replication in the periphery of the MLN during secondary infection. The inability of memory $\gamma\delta$ T cells to redistribute and cluster with replicating *L. monocytogenes* also affected the IL-17A-dependent recruitment and clustering of neutrophils with the bacteria. Accordingly, blocking both CXCR3 and IL-17A together resulted in the most significant increase in bacterial titers in the MLN following secondary *L. monocytogenes* infection. On average, a 10-fold increase in bacterial burden was observed when IL-17A alone was blocked (Fig. 3C); however, when both IL-17 and CXCR3 were blocked (Fig. 6E), we observed an average of a 22-fold increase in bacterial burden. A similar phenomenon was recently reported where CXCR3 expression on effector CD8 $\alpha\beta$ T cells was critical for their ability to migrate locally in the skin to eliminate virus-infected cells (32).

We hypothesized that the chemokines that may be critical for the guidance of neutrophils and $\gamma\delta$ Trm cells within the MLN during secondary infection could be CXCL1 and CXCL9, respectively. Indeed, we observed the compartmentalized production of CXCL1 and CXCL9 in the periphery of the LN, especially concentrated within *L. monocytogenes* replication foci. Moreover, the proper production of these chemokines was dependent on IL-17A, because antibody blocking of IL-17A markedly reduced the secretion of both CXCL1 and CXCL9, thereby impairing the formation of organized granulomatous clusters of $\gamma\delta$ Trm cells and myeloid cells, as well as the local sequestration of *L. monocytogenes* within the draining LN following secondary infection. We hypothesize that $\gamma\delta$ Trm respond to oral infection by secreting IL-17A early, which in turn induces the secretion of CXCL1 and CXCL9, forming a positive feedback loop to attract more CXCR3⁺ $\gamma\delta$ Trm cells and

myeloid cells such as neutrophils, thereby jump starting the secondary immune response to eliminate the pathogen in a timely manner. IL-17A produced by CD4 T cells may also play a role at later time points after a secondary infection. However, in our hands, blocking IL-17A clearly had important effects on the clustering and local redistribution of myeloid cells and $\gamma\delta$ T cells, but not in CD4 T-cell numbers or clustering.

Taken together, our study revealed several previously unidentified attributes of memory $\gamma\delta$ T cells. To our knowledge, this is the first report to show that $\gamma\delta$ Trm cells can establish residence in the intestinal mucosa-draining lymphoid tissue, where they produce IL-17A and thereby instruct the innate arm of the immune system to rapidly control secondary infections. Our findings illustrated how $\gamma\delta$ Trm cells mediate the choreography of local cellular migration within a secondary lymphoid organ that was essential for generating a productive antimicrobial immune response. These observations provide an exciting opportunity to design novel vaccination strategies to harness the ability of $\gamma\delta$ Trm cells to provide protection against intestinal pathogens.

Materials and Methods

Mice. Female Balb/c mice were purchased from The Jackson Laboratory and BALB/c TCR δ -H2b-eGFP mice were generated in our laboratory. All animal experiments were performed in accordance to the University of Connecticut Health Center Institutional Animal Care and Use Committee and National Institutes of Health guidelines. Additional information is provided in *SI Appendix, SI Materials and Methods*.

Infections. *L. monocytogenes* strain EGDe with recombinant InIA (11) was used for most infections. Mouse infections and bacterial burden quantitation were performed as described before (12).

For further details on all other procedures including mice strains, flow cytometric analysis, and confocal as well as multiphoton dynamic intravital imaging, see *SI Appendix, SI Materials and Methods*.

ACKNOWLEDGMENTS. We thank Dr. Lynn Puddington for helpful and critical discussion regarding the manuscript. This study was supported by NIH Grants AI95544, AI097375, and 2P01AI056172 (to K.M.K.).

- Vantourout P, Hayday A (2013) Six-of-the-best: Unique contributions of $\gamma\delta$ T cells to immunology. *Nat Rev Immunol* 13(2):88–100.
- Dunon D, et al. (1997) Ontogeny of the immune system: Gamma/delta and alpha/beta T cells migrate from thymus to the periphery in alternating waves. *J Exp Med* 186(7): 977–988.
- Carding SR, Egan PJ (2002) Gammadelta T cells: Functional plasticity and heterogeneity. *Nat Rev Immunol* 2(5):336–345.
- Haas JD, et al. (2012) Development of interleukin-17-producing $\gamma\delta$ T cells is restricted to a functional embryonic wave. *Immunity* 37(1):48–59.
- Ramirez K, Witherden DA, Havran WL (2015) All hands on DE(T)C: Epithelial-resident $\gamma\delta$ T cells respond to tissue injury. *Cell Immunol* 296(1):57–61.
- Swamy M, et al. (2015) Intestinal intraepithelial lymphocyte activation promotes innate antiviral resistance. *Nat Commun* 6:7090.
- Gebhardt T, et al. (2009) Memory T cells in nonlymphoid tissue that provide enhanced local immunity during infection with herpes simplex virus. *Nat Immunol* 10(5): 524–530.
- Sheridan BS, et al. (2014) Oral infection drives a distinct population of intestinal resident memory CD8(+) T cells with enhanced protective function. *Immunity* 40(5):747–757.
- Wu T, et al. (2014) Lung-resident memory CD8 T cells (TRM) are indispensable for optimal cross-protection against pulmonary virus infection. *J Leukoc Biol* 95(2):215–224.
- Shen Y, et al. (2002) Adaptive immune response of Vgamma2Vdelta2+ T cells during mycobacterial infections. *Science* 295(5563):2255–2258.
- Wollert T, et al. (2007) Extending the host range of *Listeria monocytogenes* by rational protein design. *Cell* 129(5):891–902.
- Sheridan BS, et al. (2013) $\gamma\delta$ T cells exhibit multifunctional and protective memory in intestinal tissues. *Immunity* 39(1):184–195.
- Ramirez-Valle F, Gray EE, Cyster JG (2015) Inflammation induces dermal Vgamma4+ $\gamma\delta$ T17 memory-like cells that travel to distant skin and accelerate secondary IL-17-driven responses. *Proc Natl Acad Sci USA* 112(26):8046–8051.
- Woodward Davis AS, Bergsbaken T, Delaney MA, Bevan MJ (2015) Dermal-resident versus recruited $\gamma\delta$ T cell response to cutaneous vaccinia virus infection. *J Immunol* 194(5):2260–2267.
- Bou Ghanem EN, et al. (2012) InIA promotes dissemination of *Listeria monocytogenes* to the mesenteric lymph nodes during food borne infection of mice. *PLoS Pathog* 8(11):e1003015.
- Matloubian M, et al. (2004) Lymphocyte egress from thymus and peripheral lymphoid organs is dependent on S1P receptor 1. *Nature* 427(6972):355–360.
- Carlson CM, et al. (2006) Kruppel-like factor 2 regulates thymocyte and T-cell migration. *Nature* 442(7100):299–302.
- Shiow LR, et al. (2006) CD69 acts downstream of interferon-alpha/beta to inhibit S1P1 and lymphocyte egress from lymphoid organs. *Nature* 440(7083):540–544.
- Mackay LK, et al. (2015) Cutting edge: CD69 interference with sphingosine-1-phosphate receptor function regulates peripheral T cell retention. *J Immunol* 194(5): 2059–2063.
- Klonowski KD, et al. (2004) Dynamics of blood-borne CD8 memory T cell migration in vivo. *Immunity* 20(5):551–562.
- Gebhardt T, et al. (2011) Different patterns of peripheral migration by memory CD4+ and CD8+ T cells. *Nature* 477(7363):216–219.
- Prinz I, et al. (2006) Visualization of the earliest steps of gammadelta T cell development in the adult thymus. *Nat Immunol* 7(9):995–1003.
- Gray EE, et al. (2013) Deficiency in IL-17-committed Vgamma4(+) $\gamma\delta$ T cells in a spontaneous Sox13-mutant CD45.1(+) congenic mouse substrain provides protection from dermatitis. *Nat Immunol* 14(6):584–592.
- Sung JH, et al. (2012) Chemokine guidance of central memory T cells is critical for antiviral recall responses in lymph nodes. *Cell* 150(6):1249–1263.
- Kastenmüller W, et al. (2013) Peripheral prepositioning and local CXCL9 chemokine-mediated guidance orchestrate rapid memory CD8+ T cell responses in the lymph node. *Immunity* 38(3):502–513.
- Guarda G, et al. (2007) L-selectin-negative CCR7- effector and memory CD8+ T cells enter reactive lymph nodes and kill dendritic cells. *Nat Immunol* 8(7):743–752.
- Schenkel JM, Fraser KA, Masopust D (2014) Cutting edge: Resident memory CD8 T cells occupy frontline niches in secondary lymphoid organs. *J Immunol* 192(7):2961–2964.
- Prinz I (2011) Dynamics of the interaction of $\gamma\delta$ T cells with their neighbors in vivo. *Cell Mol Life Sci* 68(14):2391–2398.
- Murphy AG, et al. (2014) *Staphylococcus aureus* infection of mice expands a population of memory $\gamma\delta$ T cells that are protective against subsequent infection. *J Immunol* 192(8):3697–3708.
- Schenkel JM, et al. (2014) T cell memory. Resident memory CD8 T cells trigger protective innate and adaptive immune responses. *Science* 346(6205):98–101.
- Soudja SM, et al. (2014) Memory-T-cell-derived interferon- γ instructs potent innate cell activation for protective immunity. *Immunity* 40(6):974–988.
- Hickman HD, et al. (2015) CXCR3 chemokine receptor enables local CD8(+) T cell migration for the destruction of virus-infected cells. *Immunity* 42(3):524–537.